Pillar design and the associated mining engineering constraints in hard rock bord-and-pillar mines

by W.J. Theron[1] and D.F. Malan[1]

Affiliation:
[1]Department of Mining Engineering, University of Pretoria, South Africa

Correspondence to:
D.F. Malan

Email:
francois.malan@up.ac.za

Dates:
Received: May 2024
Revised: 4 Oct. 2024
Accepted: 20 Oct. 2024
Published: November 2024

How to cite:
Theron, W.J. and Malan, D.F. 2024. Pillar design and the associated mining engineering constraints in hard rock bord-and-pillar mines. *Journal of the Southern African Institute of Mining and Metallurgy*, vol. 124, no.11, pp. 631–644

DOI:
http://dx.doi.org/10.17159/2411-9717/3413/2024

ORCiD:
D.F. Malan
http://orcid.org/0000-0002-9861-8735

Abstract

Practical mining aspects should be considered when conducting pillar designs for bord-and-pillar layouts. The current methodology for pillar design will result in increasing pillar sizes with depth. This affects the extraction ratio and will result in onerous ventilation requirements when cutting large pillars. A holistic approach, including all mining engineering requirements, is required to ensure that the rock engineering designs are optimized to ensure efficient mining operations and sustainable production. Bord widths should not only be a function of the rock mass ratings, but should also be selected to fit the specifications of the mechanized equipment. The use of a 'squat pillar' formula for hard rock is discussed in the paper and the formula based on the exponents of the Hedley and Grant pillar formula, is explored. The effect of abutments and geological losses on average pillar stress is also explored. These factors must be considered when designing layouts at increasing depths.

Keywords

pillar design, bord-and-pillar mine, mining engineering constraints, squat pillar formula

Introduction

Extensive research on the strength of hard rock pillars have been conducted and recent examples can be found in Malan and Napier, 2011; Watson et al, 2021; Napier and Malan, 2021; Oates and Malan, 2023; and Wessels and Malan, 2023. The objective of these studies is to obtain improved estimates of pillar strength to ensure stable excavations and to optimize extraction ratios. A drawback of rock engineering designs is that it is often done in isolation without including the constraints imposed by practical mining considerations. As a result, rock engineers may inadvertently design pillar sizes and layouts that may slow down production rates, decrease extraction ratios, and negatively affect productivity. An important requirement in industry is to create an awareness amongst the specialist rock engineers of the possible conflicting requirements when designing bord-and-pillar layouts. Some level of compromise is required in the final layout designs.

In general, most practical mining engineering problems require the achievement of several objectives. These may be conflicting objectives and it can therefore not be solved in isolation. For any design optimization, it is important to consider the entire mining sequence. Design is a cyclic process of evaluation, asset optimization, and system engineering. A key requirement is that a mining operation is a business with financial goals to ensure a return on investment for its shareholders. The mining value chain requires the input from various departments, namely engineering (mechanical, electrical, metallurgical), rock engineering, geology, ventilation, safety and health, environmental, human resources, procurement, and finances. When technical departments introduce a change in isolation because of immediate perceived needs, the inter-dependency of the various elements is sometimes overlooked.

Although the focus in this paper is on pillar design, a real-life practical example experienced by the authors is described below to highlight the conflicting requirements occasionally encountered. This occurred at a shallow platinum mine in the Bushveld Complex where two types of advance strike drives (ASDs) are used namely strike ASDs and normal ASDs. The width of the strike ASDs is designed to accommodate a conveyor belt and a traveling way for personnel and equipment. The normal ASDs only accommodate the travelling of personnel and equipment. A complicating factor for the excavation shape is the steep 18° dip of the strata and the hangingwall of the strike drives is profiled along the dip of the

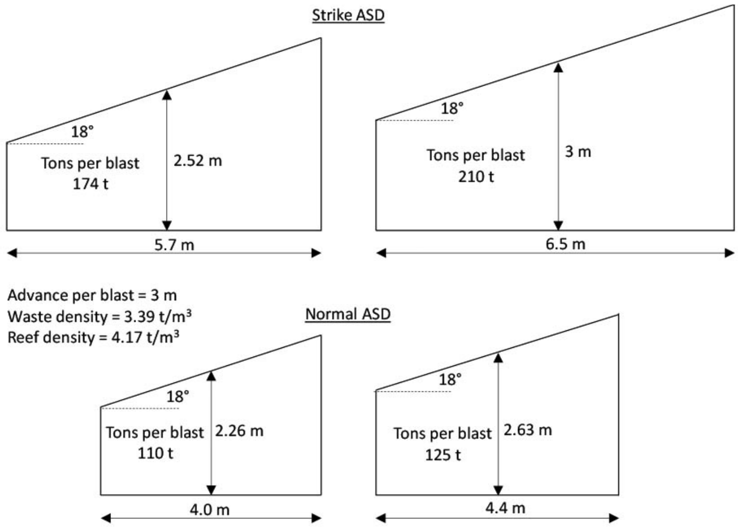

Figure 1—Changes to the strike and normal ASD excavation dimensions

strata for stability. During development blasting, the Strike ASD dimensions result in approximately 174 tons of broken rock per blast. This is calculated for a density of 4.17 t/m^3 and 3.39 t/m^3 for reef and waste, respectively, and an advance of 3 m per blast. A normal ASD results in approximately 110 tons of broken rock per blast. The dimensions of both these excavations were increased, based on an instruction from the engineering department to have greater clearances for the mechanized equipment (Figure 1). This increased the tonnage in strike ASDs to 210 tons per blast and in the normal ASD's to 125 tons per blast. A small change in dimensions therefore resulted in a significant increase in the volume of rock mined. The mine also suffered significant production losses. An activity simulation was conducted to determine the load out rate and mining cycle times with the new dimensions. Based on the input parameters in the simulation, the drilling pattern in strike ASDs could not be completed within the allowed parameters of the mining cycle. The unintended consequence of the change in clearance was a significant decrease in production.

In terms of pillar design in bord-and-pillar layouts, similar conflicting requirements can arise, owing to the current industry methodology used to design pillars. A power-law pillar strength formula of the following form is typically adopted:

$$\sigma_s = Kw^{\alpha}h^{-\beta} \qquad [1]$$

where σ_s is the pillar strength, K is the strength of the rock material in the pillar, w is the pillar width and h is the pillar height. In South Africa hard rock mines, the values 0.5 and 0.75 are typically used for the exponents α and β respectively. These values were initially adopted by Hedley and Grant (1972). A problem arises when the depth of the mines increases. The strength of the pillars as given by Equation [1] is independent of depth, but a further requirement for the design is that a minimum factor of safety, S_F, needs to be maintained. This is given by:

$$S_F = \sigma_s\left(\sigma_p\right)^{-1} \qquad [2]$$

The average pillar stress, σ_p, increases with depth for a constant extraction ratio and the factor of safety therefore decreases (Ile and Malan, 2023). Practicing rock engineers counter this by increasing the pillar width w to increase the pillar strength σ_s. This not only decreases the extraction ratio, but can also have an adverse effect on other mining engineering requirements, such as those for ventilation. Some of the mining engineering requirements are described in the following section and an interactive pillar design approach is required. Similar to the ASD example already mentioned, the unintended consequences of strictly applying Equations [1] and (2) at great depths may result in an operation not being profitable anymore. Also not considered, is that the so-called 'squat' pillar behaviour may already occur at a smaller w:h ratio for hard rock compared to coal (Ryder and Jager, 2002). Equation [1] may therefore not be applicable at the larger width to height stipulated by this traditional pillar design approach at the greater depths. Furthermore, mining engineering requirements and the need to mine profitably should also be considered at these greater mining depths. A similar conflict arises in terms of the need to introduce barrier pillars.

The sections that follow describe some important mining engineering considerations when designing bord-and-pillar layouts, namely, constraints imposed by the equipment and ventilation considerations. The paper is also used to illustrate that some of the traditional empirical rock engineering equations may not be applicable, as the original assumptions used when deriving the equations may not be valid. An important contribution of this study is the derivation of a new squat pillar formula for hard rock based on the exponents of the Hedley and Grant equation. Many practicing rock engineers in the hard rock mines do not know that the commonly used squat pillar formula is based on the Salamon coal pillar formula (Salamon, 1982).

Practical bord widths

An important mining engineering constraint when designing bord-and-pillar layouts is bord widths. Rock engineering considerations and the use of empirical design charts based on rock mass ratings will dictate a particular span (Barton, 1989; Hutchinson and Diederichs, 1996; Brady et al. 2004). The selected bord span may not be practical owing to the specifications of the available mechanized equipment. Some of the parameters used for the selection of mechanized mining equipment are mining height, required advance per blast, tons load out rates, ventilation requirements, dip of the orebody, dip of the excavations relative to the orebody, and equipment matching.

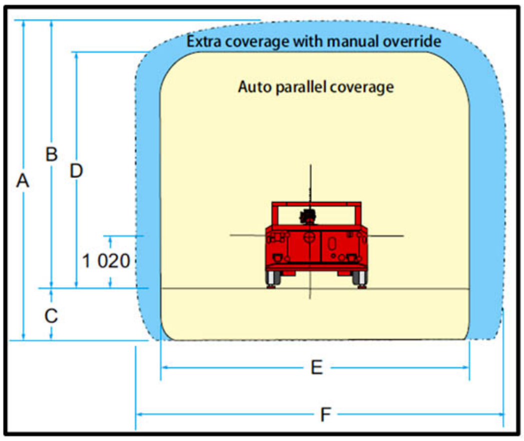

Figure 2—Diagram indicating auto parallel dimensions for drill rigs (Sandvik, 2024)

Table I

Typical generic operating dimensions for drill rigs

	A	B	C	D	E	F
Drill rig A	7 040	5 900	1 140	5 200	6 800	8 150
Drill rig B	7 040	5 900	1 140	5 200	6 180	8 150
Drill rig C	5 970	5 120	850	4 420	5 500	6 480

An equipment manufacturer will give a specification sheet based on the generic dimensions its equipment can operate in. Figure 2 and Table I give an example of the possible bord dimensions for three different types of drill rigs. Rock engineers that design layouts must be familiar with these typical constraints and the fleet of equipment available on the mine.

According to these specifications, the optimal bord width for drill rig A and B, with its auto parallel coverage function, is a maximum of 6.8 m and 6.18 m, respectively (Table I). Drill rig C is less at 5.5 m. This implies that a drill rig in a bord width with a larger dimension needs to be re-adjusted with manual override if extra coverage is required. This can typically be done in bord widths up to 8.15 m. Bord spans larger than 8.15 m will require that the rig be moved from one stationary position in the bord to another to drill all the required holes. This will adversely affect the machine efficiency and the mining cycle may not be completed in the required time. Similarly, equipment used for installing support are also specified with minimum and maximum operating dimensions, as illustrated in Figures 3 to 5.

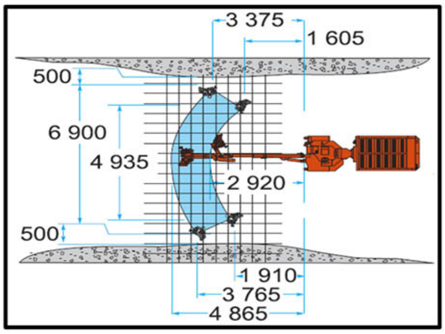

Figure 3—Roof bolter drilling boom horizontal movement path and dimensions (Sandvik, 2024)

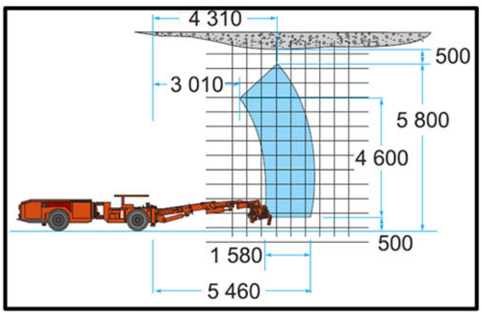

Figure 4—Roof bolter drilling boom vertical movement path and dimensions (Sandvik, 2024)

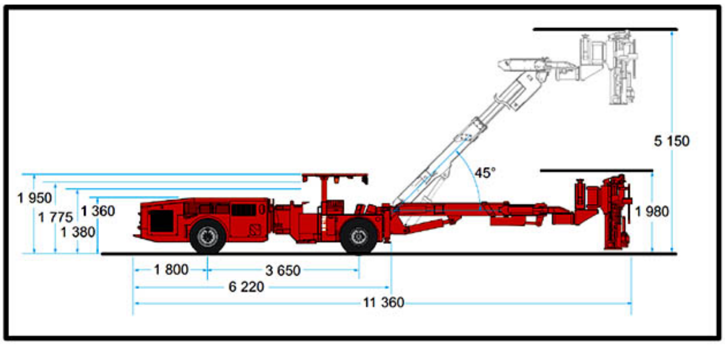

Figure 5—Roof bolter drilling boom vertical height minimum and maximum dimensions (Sandvik, 2024)

Table II

Typical bord widths and other parameters used in the South African mining industry obtained from a survey in 2020

Commodity mined	Reef type	Range of depths	Type of pillar formula	K-parameter	Pillar dimensions	Mining Height	Bord widths
Manganese	Manganese	180 m – 800 m	Hedley and Grant	133 MPa	6 m x 6 m to 8 m x 8 m	3.6 m to 5 m	8 m
Chrome	Chromitite	60 m – 330 m	Hedley and Grant	48 MPa	8 m x 8 m	2.2 m	10 m
Chrome	LG6/LG6A	35 m – 400 m	Hedley and Grant	36 MPa (0.33 *UCS)	7.5 m x 7 m (350 m depth)	2.4 m	7 m
Platinum	Merensky	850 m – 1350 m	Numerical modelling used	N/A	7 m x 7 m – 8.5 m x 8.5 m	1.8 m – 2.2 m	7 m
Platinum	UG2	Surface to 800 m	Hedley and Grant, but considering PlatMine	Third of UCS	7 m x 7 m	1.9 m – 3.5 m	8 m
Platinum	UG2	50 m – 650 m	Hedley and Grant	64 MPa	4.5 m x 4.5 m - 9 m x 9 m	2.4 m	10 m
Chrome	LG6/LG6A	30 m – 500 m	Hedley and Grant	57.5 MPa	8 m x 8 m at 410 m depth and s/w = 2.5	1.7 m – 2.5 m	6 m – 10 m
Chrome	MG1/2, LG6/LG6A	30 m – 600 m	Stacey and Page	53 MPa MG1/2 33.9 MPa LG6/6A	Varying	2 m	6 m – 10 m
Chrome	UG2	30 m – 800 m	PlatMine UG2	67 MPa PlatMine formula	Site specific	1.2 m or 2 m	Up to 14 m
Chrome	LG6/LG6A	30 m – 350 m	Hedley and Grant	2/3*UCS	6 m x 6 m to 8 m x 9 m	1.7 m to 2 m	6 m and 8 m

Based on these considerations, practical bord widths are not only a function of rock engineering considerations, but the dimensions should be matched to the capabilities of the equipment available as far as possible. An industry survey was conducted in 2020 for the SAMERDI WP4.3.1 project *(Rock engineering principles affecting the mechanization of the South African mines).* The bord widths for the various mines are shown in Table II. These dimensions vary from 6 m to 10 m and many of the mines use widths of 8 m. The efficiency of some of these mining operations can possibly be improved if the widths are better matched to the capabilities of the equipment, as discussed in the aforementioned.

Pillar widths based on rock engineering requirements

A routine problem encountered by rock engineers in the bord-and-pillar mines is to determine the optimum pillar width for an assumed factor of safety and a specified bord width. To illustrate the increase in pillar width with depth, consider the equation presented by Oates and Malan (2023). This was a calibration of the Hedley and Grant formula (Equation[1]) at a mine in the eastern Bushveld based on underground observations and numerical modelling and the equation is given by:

$$\sigma_s = 75\frac{w^{0.5}}{h^{0.75}}\ MPa = (75 \times 10^6)\frac{w^{0.5}}{h^{0.75}}\ Pa \qquad [3]$$

An iterative process is required to determine the width of the pillars for a specified factor of safety and bord width, and the general methodology is described in Wessels (2022). The relevant equation to solve for the calibrated formula in Equation [3] is derived in the following, and a practical method of solution is described. The equation derived is a useful equation as it gives the precise width of the pillars required at increasing depths. Again, it should be emphasized that practical mining engineering considerations will dictate the pillar width and it is not practical to attempt to cut a pillar with a width that includes a fraction of a meter, such as 7.341 m, although these precise dimensions can be determined by using the following equation.

The factor of safety S_F for the layout is given by Equation [2]. Tributary area theory (TAT) is commonly used to determine the average pillar stress σ_p and is given by:

$$\sigma_p = \frac{\rho g H}{1-e} \quad [4]$$

where
ρ = overburden density
g = gravitational acceleration
H = depth below surface

For square pillars and a bord-and-pillar regular layout, the extraction ratio is given by:

$$e = \frac{(w+\ell)^2 - w^2}{(w+\ell)^2} \quad [5]$$

where w is the pillar width and l is the bord and holing width (assumed to be of identical dimension). For a specified S_F, an iterative approach is required to solve for the pillar width as changes in w will affect the pillar strength in Equation [3], but also the extraction ratio in Equation [5], and therefore the average pillar stress in Equation [4]. To obtain a solution, Equation [5] can be inserted in [4]:

$$\sigma_p = \frac{\rho g H}{1 - \frac{(w+\ell)^2 - w^2}{(w+\ell)^2}} \quad [6]$$

This can be inserted in Equation [2]:

$$S_F = \frac{\sigma_s}{\rho g H}\left[1 - \frac{(w+\ell)^2 - w^2}{(w+\ell)^2}\right] \quad [7]$$

This can be rearranged to give the pillar strength.

$$\sigma_s = \frac{S_F \rho g H}{1 - \frac{(w+\ell)^2 - w^2}{(w+\ell)^2}} \quad [8]$$

This can be set equal to Equation [3]

$$(75 \times 10^6)\frac{w^{0.5}}{h^{0.75}} = \frac{S_F \rho g H}{1 - \frac{(w+\ell)^2 - w^2}{(w+\ell)^2}} \quad [9]$$

After rearranging:

$$w^{0.5}\left(1 - \frac{(w+\ell)^2 - w^2}{(w+\ell)^2}\right) = \frac{S_F \rho g H h^{0.75}}{(75 \times 10^6)} \quad [10]$$

This can be simplified to:

$$\frac{w^{2.5}}{(w+\ell)^2} = \frac{S_F \rho g H h^{0.75}}{(75 \times 10^6)} \quad [11]$$

Equation [11] was used to solve w for increasing depths. The parameters l = 8 m, S_F = 1.5, ρ = 2900 kg/m^3, g = 9.81 m/s^2 and h = 2.5 m. An interactive process is required to solve for w and a simple method to do is to use the function 'Goal Seek' in Excel. This function automatically modifies the value of w, until the left-hand side of Equation [11] is equal to the right-hand side. The calculated pillar widths for an increase in depth is given in Figure 6. Note the calculated 12 m wide pillars at a depth of a 1000 m. This can, however, be misleading and is probably not the optimum pillar design, as the large w:h ratio is not considered. Also plotted in Figure 6 is the w:h ratio. For example, for a 2.5 m mining height, a 10 m wide pillar at a depth of 800 m has a w:h ratio of 4 and the so-called 'squat' pillar behaviour needs to be considered. A squat pillar formula has never been derived for hard rock pillars in the Bushveld Complex and this is presented in Appendix A based on an approach similar to that adopted by the coal mines. Also note that the pillar design given in Figure 6 may be conservative, as tributary area theory is used and this will typically overestimate the stress acting on the pillars.

Productivity aspects related to very large pillars at depth

The analysis provided in Figure 6 indicates that the specified pillar width at depths greater than a 1000 m will exceed 12 m. These large pillars have an adverse effect on production and other mining engineering aspects. These aspects include activities such as entry examination, ventilation layout requirements, and mine production scheduling. It may be difficult to maintain a mining cycle within a shift period for very large pillars. The Mine Health and Safety Act (Act 29 of 1996) and Minerals Act (Act 50 of 1991) are prescriptive in terms of the legislative requirements imposed on mine operators and owners in South Africa. Workplaces must be safe for employees to work in and not adversely affect their health. Employers must ensure that all risks are identified and measures must be implemented to eliminate or reduce exposure to risk.

Trackless mobile machinery currently used in low profile tabular hard rock mines are mostly diesel units producing significant heat, diesel particulate matter, and carbon dioxide. To ameliorate the risks associated with the heat, gasses, dust, and diesel particulate matter, the ventilation needs to be sufficient in

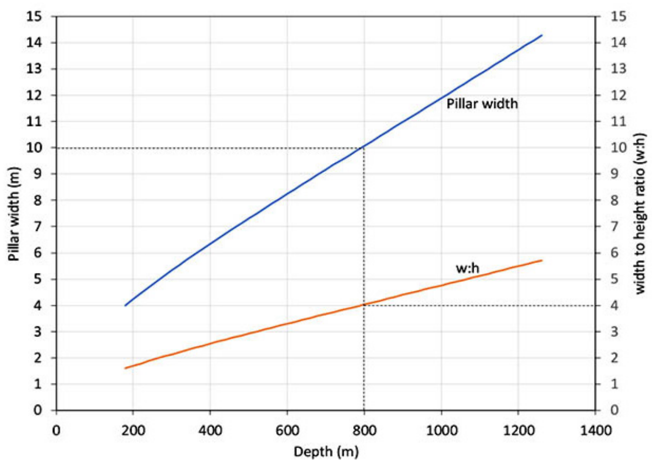

Figure 6—Calculated pillar widths versus depth and w:h ratio for the parameters listed in the text

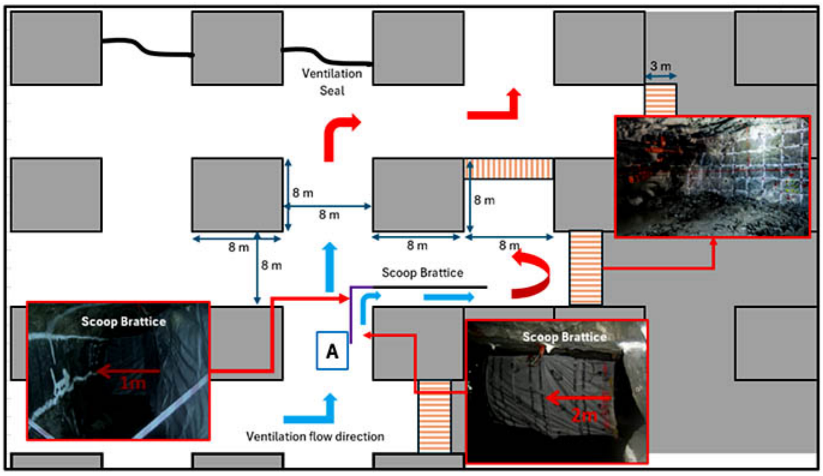

Figure 7—Required ventilation controls in an 8 m × 8 m bord-and-pillar mining layout

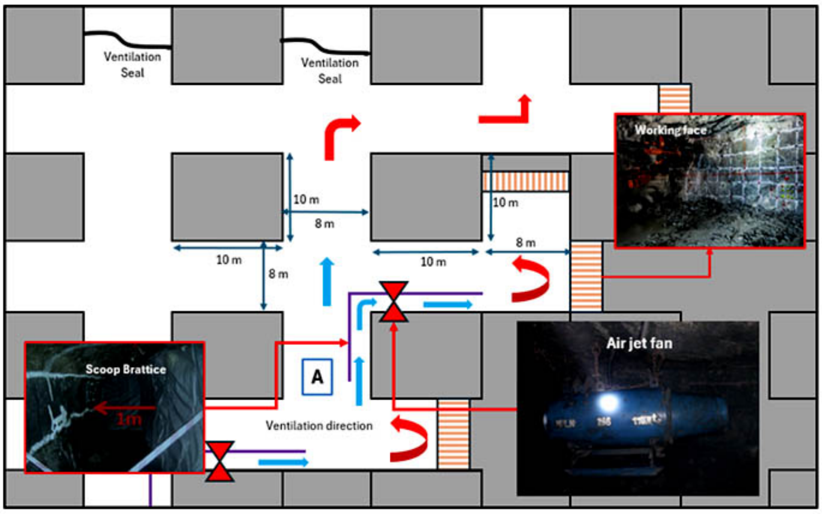

Figure 8 —Recommendation from a ventilation department to install fans to ventilate headings in a bord-and-pillar mine if the mining distance exceeds 24 m (such in the lower bord)

quantity, quality, and be directed towards the working ends. This is governed through standards and the mandatory codes of practices required by the Department of Mineral Resource and Energy in South Africa. The engine kilowatt (kW) capacity and the number of trackless mobile machinery in a mine determine the ventilation required. As an example, in one particular bord-and-pillar mine, the air volume required per rig section is 50 m^3/s, with a velocity of 0.5 m/s at the last through road from the working face. It is also required that mine personnel can only re-enter an underground workplace when the volume of air in the area has been replaced 8 times to ensure that all harmful gases are removed. This period is termed the re-entry time. Entry examination occurs after the re-entry period and it is a critical procedure prior to any other mining activities to ensure that all risks are addressed in a working place and the area is declared safe. The entry examination starts with measuring all ventilation requirements as no work can commence if the environmental conditions are sub-standard and hence, unsafe for employees. Larger pillars require larger distances to be mined before the pillars can be cut to establish the next ventilation holing. This has implications in terms of maintaining adequate ventilation conditions in the workplaces and will require ventilation controls in the form of scoop brattices, ventilation seals, and other mechanical means of ventilating. Examples from one particular mine is illustrated in Figures 7 and 8. This illustrates the more onerous requirement for 10 m (or larger) pillars versus 8 m wide pillars.

Figure 7 illustrates that, when an advancing working face progress beyond 16 m from the last through ventilation roadway (indicated by 'A'), a ventilation control named a 'scoop brattice' will be required. This direct ventilation flows towards the working face to maintain the required ventilation conditions. This additional control will be adequate for up to 24 m. This allows for the next pillar holing to be holed through, reducing the need for additional ventilation controls.

Figure 8 illustrates that, as the advancing faces progress beyond a distance of 24 m because of increased pillar sizes, additional ventilation controls such as 11 kW air jet fans, will be required to meet the ventilation requirements. Pillar sizes beyond 10 m will require ventilation controls similar to those used in mining development ends consisting of a combination of 75-kW, 45kW,- and 22.5-kW booster fans with a range of different diameter ventilation columns for each, with various delivery and pick-up positions to prevent recirculation. This means additional employees

Table III

Drill rig operator critical path-based activities and duties per shift

Task	Time
Pre-shift machine inspection.	30 min
Refuel machine at underground refueling location.	20 min
Tram to the nearest electrical point for electrical connection needed.	20 min
Park machine safely and connect machine to electrical point.	10 min
Tram to face / bord planned for drilling.	10 min
Park and position machine safely and correctly for drilling.	10 min
Suspend 70 m electrical cable to hanging wall as required.	15 min
Connect drilling water and establish water pumping arrangements.	10 min
Actual drilling time per bord based on bord width – An operator is required to complete two faces / bords per shift.	6 m – 2h08 min 8 m – 2h42 min 10 m – 3h19 min
Tram machine to wash bay after drilling activity complete.	20 min
Wash machine and report at end of shift.	30 min

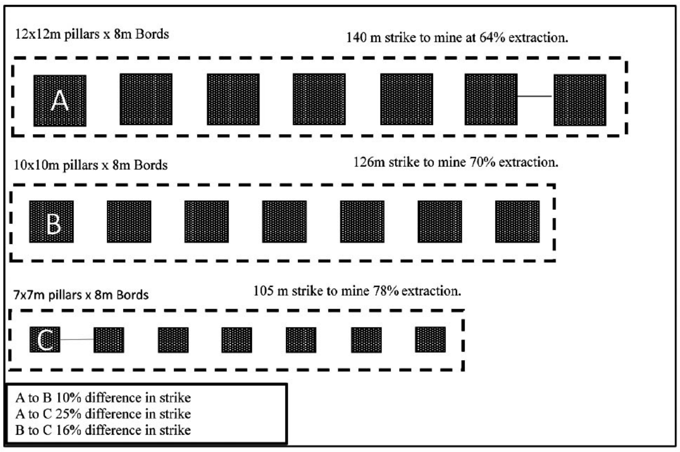

Figure 9—A comparison of strike mining distances for different pillar sizes

per stoping crew resulting in reduced efficiencies. The larger the pillars are, the more onerous the ventilation controls become and the more time it will take to complete a full mining cycle. This will lead to reduced productivity levels.

Mining operations consist of an activity sequence that works in series and an activity can only start when the preceding activity is fully completed. For example, the workers can only drill a working face when all required support in that workplace has been completed. They can only charge up that face with explosives when the drilling is completed. To illustrate the typical times, a drill rig operator's daily duties are given in Table III.

The average times are derived from using a Sandvik DD210L single-boom electro-hydraulic development drill rig designed for underground mining. Key specifications include a coverage area of 36 m^2, a hole length of up to 3.5 m, and a hole diameter range of 43 to 64 mm. An operator needs 5.2 hours to drill just one working face that is 6 m wide, 5.6 hours for an 8 m wide excavation and 6.2 hours for a 10 m wide excavation. An operator is required to complete two working faces in a shift duration of 10 hours to meet productivity output parameters. Any additional requirements inhibiting the operator from utilizing the full shift hours available will result in the second end not to be completed in time.

Smaller pillars imply reduced meters advance required to affect holings, reducing additional ventilation control requirements and reduced time to declare working areas safe. This result in improved productivity efficiencies and cost benefits. A further benefit of using the smallest possible pillar size is that a larger overall extraction rate can be achieved (see Figure 9). Substantial additional revenue can be generated as the orebody is more efficiently mined. Some mines may argue that they have large reserves and therefore reducing the pillar sizes are not important. This approach is not acceptable as the onus is on the mining industry to exploit the orebodies optimally. The highest possible extraction ratio, which will still ensure stable excavations, needs to be adopted.

Smaller pillars and a higher extraction ratio reduce the required advance rate in the strike direction. It therefore takes longer to mine to the boundaries (see Figure 9). This is beneficial to the engineering department as there is less pressure to advance the conveyors on strike with associated labour and cost benefits. The conveyors can be kept close to the mining faces, reducing tramming time and resulting in less wear and tear on the mining equipment. Smaller pillars also increase the life of mine, as one maximizes the available resource that can be economically extracted, providing significant benefits for communities and society at large.

Squat pillar behaviour in hard rock mines

Considering the mining engineering preference for smaller pillars discussed in the aforementioned, a careful study of the pillar design methodology is required. As shown in Section 3, the application of the Hedley and Grant formula in mines in the Bushveld Complex may result in a too conservative design if consideration is not given to the width to height (w:h) ratio of the pillars.

Regarding the strength of squat pillars, the original coal pillar database used by Salamon and Munro (1967) contained no pillar with a width to height ratio greater than 3.8. Evidence collected in the field suggested that, beyond a critical width to height ratio, the pillar strength exceeds that suggested by the simple power-law formula given in Equation [1]. Salamon (1982) therefore proposed that, when the width to height ratio exceeds a critical ratio, the pillar strength formula should be replaced by the following squat formula for coal pillars:

$$\sigma_{coal} = KV^{-0.0667}R_0^{0.5933}\left\{\frac{0.5933}{\varepsilon}\left[\left(\frac{R}{R_0}\right)^{\varepsilon} - 1\right] + 1\right\} \qquad [12]$$

where
K = the strength of a unit cube of coal
V = the pillar volume (m³)
R = the pillar width to height ratio
R_0 = the critical width to height ratio
ε = rate of pillar strength increase

From field data, no evidence was available of a collapse of a pillar with a width to height ratio greater than 4. Therefore, the critical width to height ratio was arbitrarily selected as 5. A value of 2.5 was chosen for ε as it was considerably lower than that obtained from laboratory tests on sandstone.

Interestingly, if $R = R_0$, Equation [12] can be simplified as

$$\sigma_{coal} = KV^{-0.0667}R_0^{0.5933} \qquad [13]$$

and this is equivalent to the Salamon and Munro (1967) equation (Equation [A1], Appendix A) with values $\alpha = 0.46$ and $\beta = 0.66$. At the critical width to height ratio (R_0), the strength predicted by the coal squat pillar is therefore similar to that predicted by the Salamon power-law equation.

In the absence of any other equation, rock engineers in the hard rock mines of the Bushveld Complex often use Equation [12]. It should be considered that this equation was derived for coal pillars and its application to hard rock pillars can be questioned, as it was based on the coal pillar strength formula.

A further difficulty with this equation is that several assumptions need to be made and it is onerous to determine the rate of pillar strength increase (ε) and the critical width to height ratio (R_0). Over the years, some criticism has been raised about the complexity of the need to combine the power-law equation and the squat pillar equations at an almost arbitrary w:h ratio. Ryder and Jager (2002) described it as follows: "*Virtually all laboratory and field evidence indicates that the w:h strengthening curve actually has zero or positive upward curvature throughout – Figure 10. Yet, by its very structure, the power formula forces downward curvature on the fitted characteristic – dashed curve, Figure 10. This in turn forces the inelegant form of the 'squat pillar formula'*".

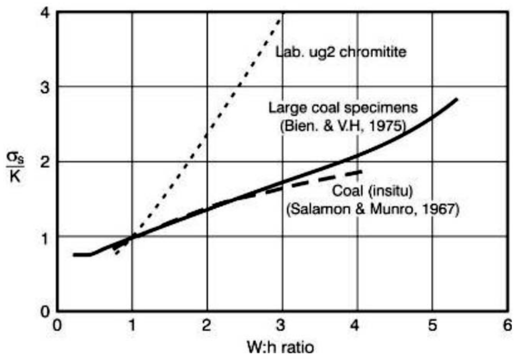

Figure 10—Laboratory and in-situ strengths of pillars for increasing w:h ratios (after Ryder and Jager, 2002)

If the same approach is followed for the Hedley and Grant equation, the equivalent squat pillar formula for hard rock using the Hedley and Grant exponents can be derived as (see Appendix A):

$$\sigma_{hard\ rock} = KV^{-0.0833}R_0^{0.6667}\left\{\frac{0.6667}{\varepsilon}\left[\left(\frac{R}{R_0}\right)^{\varepsilon} - 1\right] + 1\right\} \qquad [14]$$

The same rate of pillar strength increase is assumed for hard rock (ε = 2.5) as for coal, which may be too conservative, but a smaller critical width to height ratio of 3 is deemed more appropriate for the onset of squat pillar behaviour. The motivation for this is as follows: Ryder and Jager (2002) noted that the onset of squat behaviour is significantly earlier for hard rock pillars than the w:h ratio of 5 adopted for coal pillars. Zipf (2001) also noted that the w:h ratios of pillars are always less than 3 for coal mine failures, usually much less than 1 in metal-mine failures, and less than about 2 for non-metal mine failures. An assumption of R_0 = 3 for the UG2 pillars may therefore still be conservative. Based on these assumptions, Equation [14] can be used to estimate the strength of a 10 m wide UG2 pillar with a height of 2.5 m as:

$$\sigma_{UG2} = 75 \cdot 250^{-0.0833}3^{0.6667}\left\{\frac{0.6667}{2.5}\left[\left(\frac{4}{3}\right)^{2.5} - 1\right] + 1\right\} MPa = 126\ MPa \qquad [15]$$

For the Hedley and Grant equation with K = 75 MPa, the

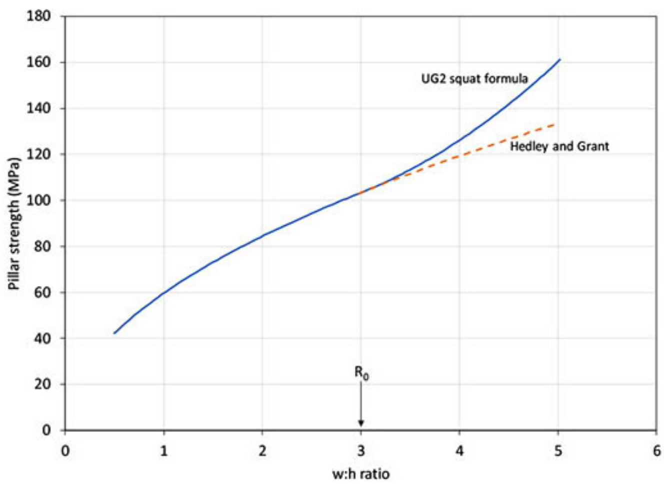

Figure 11—Predicted strength of UG2 pillars using the combined Hedley and Grant formula and the squat formula for K = 75 MPa. The strength was calculated for a pillar height of 2.5 m. This is plotted for R_0 = 3

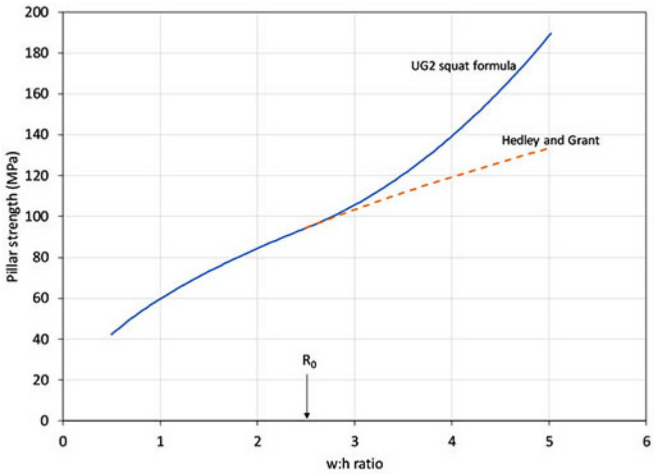

Figure 12—Predicted strength of UG2 pillars using the combined Hedley and Grant formula and the squat formula for K = 75 MPa. The strength was calculated for a pillar height of 2.5 m. This is plotted for $R_0 = 2.5$

predicted strength for a 10 m wide pillar is 119 MPa and the squat pillar formula therefore predicts that the 10 m wide pillar will be approximately 5% stronger. This is, however, based on the unverified assumptions and is only a first order estimate.

The combined Hedley and Grant and squat pillar strength for the UG2 is illustrated in Figure 11. Note that the upward curve in strength may start earlier than shown. This is for the adopted value of $R_0 = 3$. Figure 12 illustrate the curves for of $R_0 = 2.5$. Clearly the predicted strength will be significantly affected by the choice of R_0.

There is not a significant difference between the coal and hard rock equations given in Equations [12] and [14]. This is to be expected as the exponents in the Salamon and Munro coal and Hedley and Grant hard rock formulae are not significantly different. These two squat pillar equations are compared in Figure 13 for w:h ratios between 3 and 5. Identical parameters are used in both equations namely K = 75 MPa, $R_0 = 3$, $\varepsilon = 2.5$ and $h = 2.5$ m. Note that the coal squat pillar formula predicts a slightly lower strength. The predicted pillar strength will be more affected by the choice of R_0.

Figures 11 and 12 highlight a very important aspect in terms of pillar design as part of the mining value chain. The uncertainty in the onset of squat pillar behaviour ($R_0 = 2.5$ or $R_0 = 3.0$) can result in significantly different pillar sizes. Faced with this uncertainty, rock engineers will invariably choose the conservative design and this may have an adverse effect on other aspects, such as the need for onerous ventilation requirements when cutting large pillars. There is therefore a need to critically examine the design criteria and the necessary studies and experimentation need to be done to obtain improved design methodologies. As an important cautionary note, Equation [14] needs to be tested using appropriate underground trial sites and monitoring. Furthermore, the uncertainty regarding the application of the coal squat pillar formula was highlighted by Mathey and Van der Merwe (2016), and these formulae should be used with caution.

The effect of barrier pillars and geological losses

Barrier pillars result in similar production constraints caused by large in-panel pillars. Use of these barrier pillars detrimentally affects the extraction ratio and time required to open new mining blocks. Some general rules for the introduction of barrier pillars

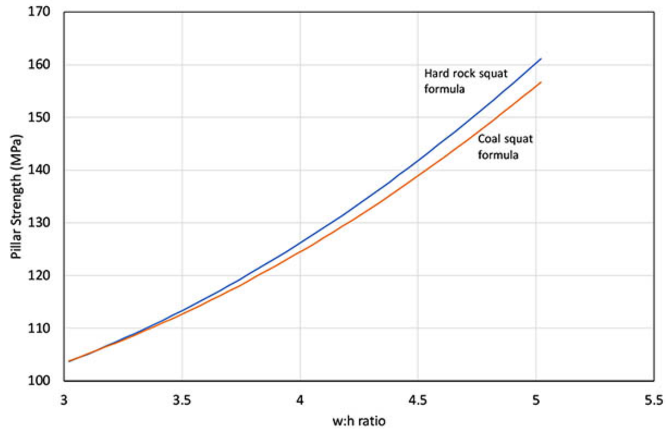

Figure 13—Comparison between hard rock squat pillar formula and the coal squat formula

are given by Ryder and Jager (2002). There is not a good technical motivation for these pillars if the factor of safety is high on the in-panel pillars. It is stated in Ryder and Jager (2002): '*It follows that the old '1/4 depth' rule of thumb (that is, that the regional span:depth ratio should not exceed 1/4) is overly conservative if in-panel pillars are in place, and indeed regional pillars may not be necessary at all in the presence of strong in-panel pillars. Nevertheless, it is recommended that regional pillars be maintained as 'barriers', but at S/H ratios up to about ½.*'. Interestingly, it is stated the '*regional pillars may not be necessary at all*', but then it is recommended that it should be used anyway. This may result in an unjustified reduction in extraction ratio. Furthermore, potholes already cause substantial losses in some areas, especially when mining the UG2 reef. No attempt has been made to include these geological losses as part of regional pillar design. The in-pillar designs for the UG2 reef may possibly be rather conservative as a result.

Some understanding of the spatial distribution of potholes will be required to consider their possible use as part of a barrier pillar system for a new layout design. Chitiyo et al. (2008) describe the predictability of pothole characteristics and their spatial distribution at the Rustenburg Platinum Mine. They note that: '*Prediction of pothole characteristics is a challenging task, confronting production geologists at the platinum mines of the Bushveld Complex. The frequency, distribution, size, shape, severity and relationship (FDS3R) of potholes has a huge impact on mine planning and scheduling, and consequently cost.*' Their quantitative analysis of potholes indicates that pothole size can be described by two partly overlapping lognormal distributions. They referred to these as Populations A (< 20 m diameter) and B (20-500m diameter). A third size range of very large potholes can be found and these were referred to as Population C (> 1 km in diameter). They state that for the UG2, Population A potholes are generally randomly distributed and clustered, whereas Population B potholes are randomly distributed with less clustering. The authors do not describe how they defined 'clustering' of the potholes, however. They also note that potholes are quasi- circular with a minor tendency of elongation. In the UG2, potholes with elongated forms are more prevalent in the size range 20 m – 500 m diameter. In summary, this previous study indicates that in both the UG2 and the Merensky Reef, the potholes are randomly distributed, with a tendency towards clustering. Clustering appears to be more prevalent in the smaller Population A potholes. No suitable proxy could be found for the prediction of UG2 pothole density and, according to the authors, these are best predicted by extrapolation of the known pothole density.

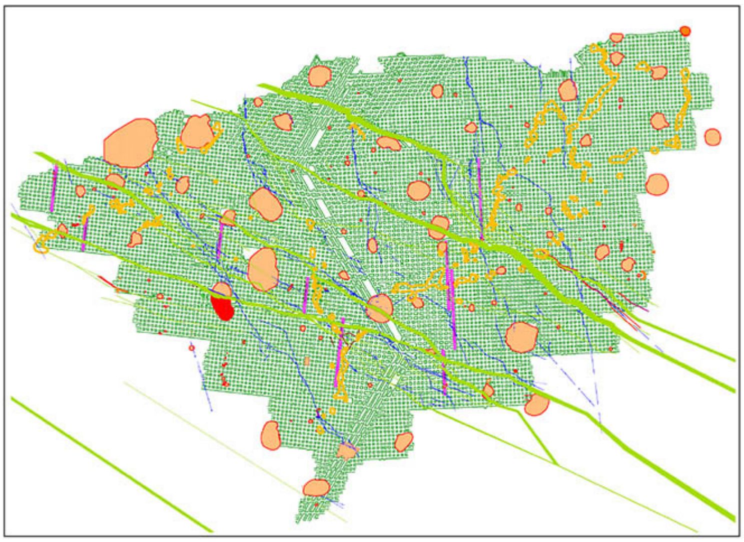

Figure 14—The distribution of potholes and dykes on the UG2 reef horizon at a mine in the eastern Bushveld

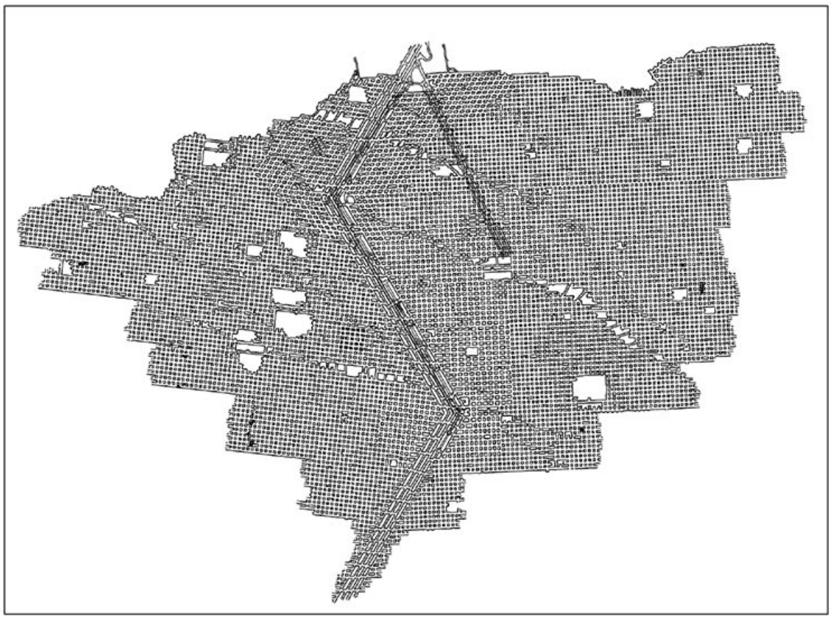

Figure 15—The remaining pillars for the mine illustrated in Figure 14

The distribution of potholes and other geological structures on the UG2 reef horizon at a mine in the eastern Bushveld are illustrated in Figure 14. Note the high density of these structures and it is clear that a tributary area theory assumption for the in-panel pillar stress will overestimate the average pillar stress (σ_p) values. Also, of significance is the light green dykes traversing the orebody. Only strategic development ends are mined through the dykes and potholes and these include important roadways, strike belts, and ventilation ends. The dykes will therefore also reduce the extraction ratio and reduce the stress on some of the in-panel pillars. The actual layout and the many regional pillars are shown in Figure 15.

The total pothole area for Figure 14 was calculated as 191 480 m^2 and the total mine area, including the pillars and geology, as shown in Figure 15 is 2 629 761 m^2. This implies that the extraction ratio is a maximum of 92.7%. It should be noted, however, that this is a conservative calculation of the extraction ratio as all the other large pillars (e.g., the decline pillars and the dykes) were not considered. Recent figures obtained from the mine provided a worse extraction ratio. The total mine area, including pillars, is 3 150 589 m^2, while the mined area is only 2 169 789 m^2. This provides an overall extraction ratio of only 68.9%. It will therefore not be beneficial to introduce an additional barrier pillar system, as the average pillar stress (σ_p) values will be lower than that predicted by tributary area theory (TAT).

Although it is known that TAT is a conservative approach to estimate σ_p values and that abutments will reduce σ_p, the effect of different spans on σ_p has never been quantified. A number of modelling runs on square layouts with different mining spans were therefore conducted for this study using the TEXAN code (Napier and Malan, 2007). A layout of 7 m wide pillars and 8 m wide bords were used for all the simulations. The key objective was to determine if the proximity of abutments will affect the peak and average pillar stress in the mining areas.

Table IV
Square geometries simulated

Geometry	Pillar width (m)	Bord width (m)	Total pillars	Span (m)	Total area (m²)
3 x 3 pillars	7	8	9	53	2 809
4 x 4 pillars	7	8	16	68	4 624
5 x 5 pillars	7	8	25	83	6 889
7 x 7 pillars	7	8	49	113	12 769
10 x 10 pillars	7	8	100	158	24 964
14 x 14 pillars	7	8	196	218	47 524
20 x 20 pillars	7	8	400	308	94 864
25 x 25 pillars	7	8	625	383	146 689
30 x 30 pillars	7	8	900	458	209 764

Table V
APS values predicted by TAT for the depths simulated

Depth (m)	Pillar width (m)	Bord width (m)	Extraction ratio	TAT APS (MPa)
200	7	8	0.782	28.47
400	7	8	0.782	56.94
600	7	8	0.782	85.41

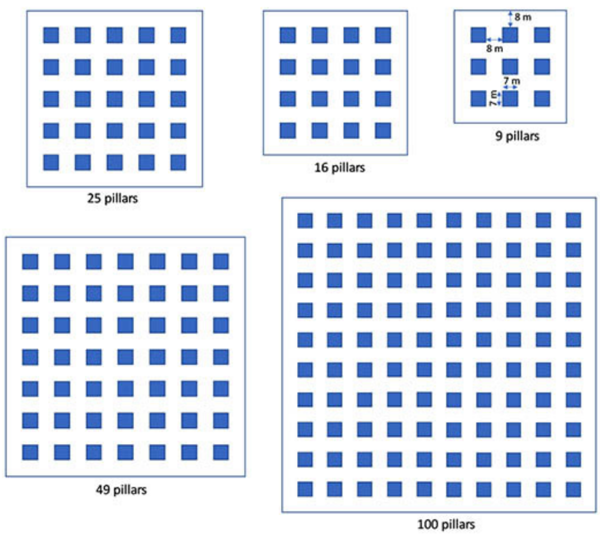

Figure 16—The smaller square geometries simulated

The geometries simulated are illustrated in Figures 16 and 17. The parameters of the various layout sizes are also summarized in Table IV. All geometries were simulated at depths of 200 m, 400 m, and 600 m. The simulations were also conducted with the TEXAN code. The parameters used were Young's modulus = 70 GPa, Poisson's ratio = 0.2, and an overburden density = 3100 kg/m³. The TAT values at the three depths simulated are provided in Table V. Square elements with a size of 1 m were used. Each pillar therefore consisted of 49 elements and the largest model span required the use of 209 764 elements. For each of the simulations, the peak APS as

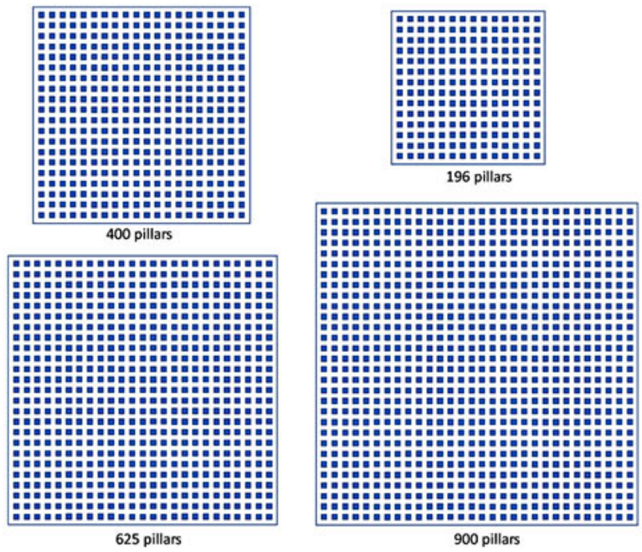

Figure 17—The larger square geometries simulated

well as the average APS of all the pillars (except for the three largest spans) were computed. As expected, both the peak and average APS values increased as the span increased.

A study of the simulated data indicated that the peak APS and average APS as a function of the mining area can be simulated with the following empirical equations (these were derived for this study):

$$\sigma_{peak} = TAT\left[1 - \gamma\left(\frac{A}{A_0}\right)^{-\delta}\right] \quad [16]$$

$$\sigma_{ave} = TAT\left[1 - \omega\left(\frac{A}{A_0}\right)^{-\eta}\right] \quad [17]$$

where
σ_{peak} = peak σ_p in the centre of the square mining area
σ_{ave} = average σ_p of all the pillars in the square mining area
TAT = σ_p predicted by tributary area theory
A = total area mined
A_0 = tributary area (unit cell of the geometry)
$\gamma, \delta, \omega, \eta$ = constants

Table VI
Calibrated parameters for the empirical stress equations for the 'infinite' depth simulations

Depth (H)	A_0	ρ	g	e	γ	δ	ω	η
200 m	225 m^2	3100 kg/m^3	10 m/s^2	0.782222	0.7610	0.5138	0.5810	0.3133
400 m	225 m^2	3100 kg/m^3	10 m/s^2	0.782222	0.7590	0.5128	0.5859	0.3146
600 m	225 m^2	3100 kg/m^3	10 m/s^2	0.782222	0.7581	0.5122	0.5802	0.3127

The TAT value is given by Equation [4] and this can be inserted to give:

$$\sigma_{peak} = \frac{\rho g H}{(1-e)}\left[1 - \gamma\left(\frac{A}{A_0}\right)^{-\delta}\right] \quad [18]$$

$$\sigma_{ave} = \frac{\rho g H}{(1-e)}\left[1 - \omega\left(\frac{A}{A_0}\right)^{-\eta}\right] \quad [19]$$

Note that in the limit if A → ∞, the values correctly tend to the TAT value:

$$\lim_{A\to\infty} \sigma_{peak} = \frac{\rho g H}{(1-e)} \quad [20]$$

$$\lim_{A\to\infty} \sigma_{ave} = \frac{\rho g H}{(1-e)} \quad [21]$$

The results for the different areas and the three depths are illustrated in Figures 18 to 20. Note that the newly derived empirical models in Equations [18] and [19] provide a very good fit with the numerical models. The simulated values are less than the TAT value in each case. It correctly predicts that as the area increases in sizes, the values tend to the TAT value. The peak APS value for all three depths is 98% of the TAT value for the largest mined area of 209 764 m^2. In comparison, the σ_{ave} of all pillars in the simulated area is substantially lower than the TAT value. The question should be posed if the pillar designs should not be rather done by using this σ_{ave} value. Note that the σ_{ave} values were not calculated for the largest two geometries owing to the lack of an automated post processor for TEXAN and the onerous task of finding and averaging the correct pillar elements for 900 pillars in a data dump of 209 764 elements.

The calibrated parameters for Equations [18] and [19] are given in Table VI. The method of least squares was used to find the calibrated values of γ, δ, ω, and η. This can be easily done by using the 'Solver' add-in utility in Excel. Interestingly, the calibrated values are essentially similar for the various depths.

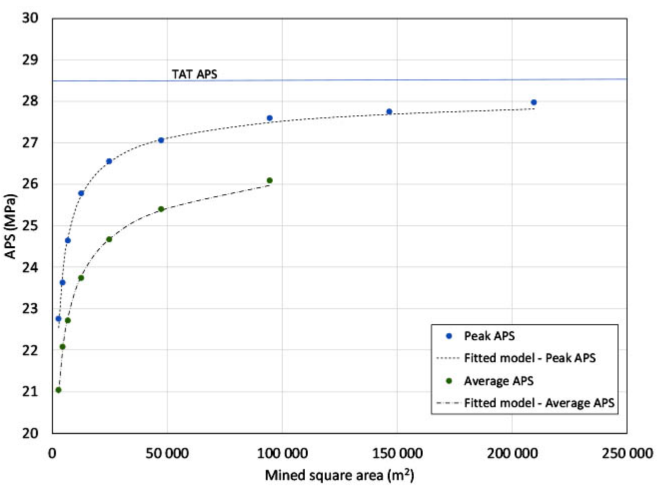

Figure 18—Simulated peak and average APS values for the square layouts of increasing size at a depth of 200 m

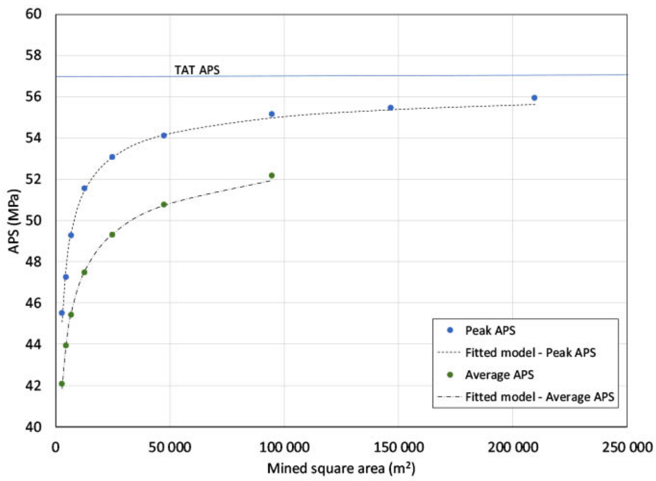

Figure 19—Simulated peak and average APS values for the square layouts of increasing size at a depth of 400 m

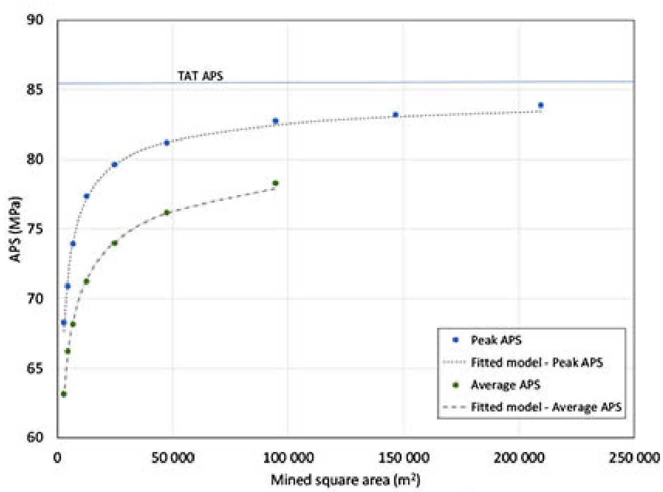

Figure 20—Simulated peak and average APS values for the square layouts of increasing size at a depth of 600 m

In summary, it is clear from this modelling that abutments and geological losses will result in average pillar stresses that can be substantially smaller than that predicted by TAT. Designs not considering these effects will likely be too conservative and will result in an unnecessary additional reduction in extraction ratio and an increase in pillar sizes. Numerical modelling can assist with these designs to estimate more realistic stress magnitudes acting on the pillars. It is important in future that rock engineering designs are not only based on historic methodologies and empirical equations that may not always be applicable. Rock engineers should question the methodologies, establish trial sites, and monitor the rock mass behaviour to search for methods to optimize designs. The sentiment expressed by Franklin (1977) is still applicable today:

'*One solution for design based on uncertain data is to adopt a conservative approach with correspondingly high factors of safety. A better alternative is to recognize that much of the design work must be done in the course of execution of the project based on observations of actual rock conditions and on the records obtained by monitoring.*'

Conclusions

This study highlighted the importance to include practical mining considerations when conducting pillars designs for bord-and pillar-layouts. Mechanized equipment, such as drill rigs, are designed to function best when bord widths are restricted to a particular dimension and, if possible, the rock engineering designs should accommodate this. Large pillars should preferably be avoided at great depths, as this will result in onerous ventilation requirements and poor efficiencies when cutting these pillars. Extremely large pillars may in fact not be required at great depth owing to the squat pillar behaviour of these pillars. A squat pillar formula for hard rock pillars based on the exponents of the Hedley and Grant formula, is discussed in the paper. This work needs to be verified in future using experimental studies. Estimating pillar stress is a further important aspect of pillar design. It is clear from the modelling conducted in the study that abutments and geological losses will result in average pillar stresses that can be substantially smaller than that predicted by TAT. Numerical modelling should be used to estimate more realistic stress magnitudes acting on the in-panel pillars. Stress measurements should also be conducted to verify these modelling results.

Acknowledgements

This work forms part of the M Eng (Mining Engineering) study of Mr Willie Theron at the University of Pretoria. The authors would like to thank Northam Platinum for their permission to publish this information. The assistance provided by Noel Fernandes is greatly acknowledged.

References

Barton, N. 1989. Cavern design for Hong Kong rocks, In AW Malone & PGD Whiteside (eds), Rock cavern –Hong Kong. *The Australasian Institute of Mining and Metallurgy*, Melbourne, pp. 179–202.

Brady, T., Martin, L., Pakalnis, R. 2004. Empirical approaches for opening design in weak rock masses. *National Institute of Occupational Safety and Health*, United states of America. https://stacks.cdc.gov/view/cdc/8691

Chitiyo, G., Schweitzer, J., De Waal, S., Lambert, P., Olgilvie, P. 2008. Predictability of pothole characteristics and their spatial distribution at Rustenburg Platinum Mine. *Journal of the Southern African Institute of Mining and Metallurgy*, vol. 108, no. 12, pp. 733–740.

Franklin, J.A. 1977. The monitoring of structures in rock. *International Journal of Rock Mechanics and Mining Sciences & Geomechanics Abstracts*, vol. 14, no. 4, pp. 163–192. https://doi.org/10.1016/0148-9062(77)90947-0

Hedley, D.G.F., Grant, F. 1972. Stope-and-pillar design for the Elliot Lake Uranium Mines. *Canadian Institute of Mining and Metallurgy* vol. 65, pp. 37–44.

Hutchinson, D.J., Diederichs, M.S. 1996. Cable Bolting in Underground Mines. Richmond: BiTech Publishers.

Ile, D., Malan, D.F. 2023. A study of backfill confinement to reinforce pillars in bord and pillar layouts. *Journal of the Southern African Institute of Mining and Metallurgy*, vol. 123, no. 5, pp. 223–234. http://dx.doi.org/10.17159/2411-9717/2452/2023

Malan, D.F., Napier, J.A.L. 2011. The design of stable pillars in the Bushveld mines: A problem solved? *Journal of the Southern African Institute of Mining and Metallurgy*, vol. 111, pp. 821–836.

Mathey, M., Van der Merwe, J.N. 2016. Critique of the South African squat coal pillar strength formula. *Journal of the Southern African Institute of Mining and Metallurgy*, vol. 116, pp 291–299. https://dx.doi.org/10.17159/2411-9717/2016/v116n3a11

Napier, J.A.L. and Malan, D.F. 2007. The computational analysis of shallow depth tabular mining problems. *Journal of the Southern African Institute of Mining and Metallurgy*, vol. 107, pp. 725–742.

Napier, J.A.L., Malan D.F. 2021. A limit equilibrium model of tabular mine pillar failure. *Rock Mechanics and Rock Engineering*, vol. 54, pp. 71–89. https://dx.doi.org/ 10.1007/s00603-020-02265-2

Oates, T., Malan, D.F. 2023. A study of UG2 pillar strength using a new pillar database. *Journal of the Southern African Institute of Mining and Metallurgy*, vol. 123, no. 5, pp. 265–274. http://dx.doi.org/10.17159/2411-9717/2656/2023

Ryder, J.A., Jager, A.J. 2002. *A textbook on rock mechanics for tabular hard rock mines. Johannesburg: SIMRAC.*

Salamon, M.D.G., Munro, A.H. 1967. A study of the strength of coal pillars. *Journal of the South African Institute of Mining and Metallurgy*, vol. 68, pp. 56–67.

Salamon, M.D.G. 1982. Unpublished Report to Wankie Colliery.

Sandvik. 2024. Underground Drill Rigs. Retrieved from www.rocktechnology.sandvik

Watson, B.P., Theron, W., Fernandes, N., Kekana, W.O., Mahlangu, M.P., Betz, G., Carpede, A. 2021. UG2 pillar strength: Verification of the PlatMine formula. *Journal of the Southern African Institute of Mining and Metallurgy*, pp. 449–456. http://dx.doi.org/10.17159/2411-9717/1491/2021

Wessels, D.G. 2022. A review of the pillar design methodology for manganese mining operations in South Africa, M Eng dissertation, University of Pretoria.

Wessels, D.G., Malan, D.F. 2023. A limit equilibrium model to simulate time-dependent pillar scaling, *Rock Mechanics and Rock Engineering*, vol. 56, pp. 3773–3786. http://dx.doi.org/10.1007/s00603-023-03239-w

Zipf, R.K. 2001. Toward pillar design to prevent collapse in room-and-pillar mines. *108th Annual Exhibit and Meeting, Society for Mining, Metallurgy and Exploration*, Krakow, Poland, Jun 2001. ◆

Appendix A

Derivation of a squat pillar formula for hard rock

The power-law strength formula is given by:

$$\sigma_s = K\frac{w^\alpha}{h^\beta} \quad \text{[A1]}$$

where K reflects the 'strength' of the in-situ rock, w is the width of the (square) pillar and h is the height in meters. The pillar volume V is given by

$$V = w^2h \quad \text{[A2]}$$

The width:height ratio is given by R:

$$R = \frac{w}{h} \quad \text{[A3]}$$

Rewrite Equation [A2]:

$$h = \frac{V}{w^2} \quad \text{[A4]}$$

Rewrite Equation [A3]:

$$w = Rh \quad \text{[A5]}$$

Insert [A4] in [A5] and rearrange

$$w = (RV)^{\frac{1}{3}} \quad \text{[A6]}$$

Insert [A6] in [A4] and rearrange

$$h = \frac{V}{(RV)^{\frac{2}{3}}} \quad \text{[A7]}$$

When inserting [A6] and [A7] in [A1]:

$$\sigma_s = K\frac{(RV)^{\frac{\alpha}{3}}}{\left[\frac{V}{(RV)^{\frac{2}{3}}}\right]^\beta} \quad \text{[A8]}$$

This can be simplified as

$$\sigma_s = K\frac{(RV)^{\frac{\alpha}{3}+\frac{2\beta}{3}}}{(V)^\beta} \quad \text{[A9]}$$

and further as

$$\sigma_s = K\left(R^{\frac{\alpha}{3}+\frac{2\beta}{3}} \cdot V^{\frac{\alpha}{3}+\frac{2\beta}{3}-\beta}\right), \quad \text{[A10]}$$

which is similar to Equation [12] in the text

$$\sigma_s = KV^{(\alpha-\beta)/3}R^{(\alpha+2\beta)/3} \quad \text{[A11]}$$

For Hedley and Grant, $\alpha = 0.5$ and $\beta = 0.75$ and Equation [A11] becomes:

$$\sigma_{HG} = KV^{-0.0833}R^{0.6667} \quad \text{[A12]}$$

This form of the equation was extended by Salamon (1982) by adding a simple power law function of the ratio of the pillar width to height ratio (R) to the critical width to height ratio (R_0). The exponent is the rate of pillar strength increase (ε). Salamon selected the following constant as the width of the scaling relationship of the power law:

$$\frac{(\alpha+2\beta)/3}{\varepsilon} \quad \text{[A13]}$$

If these assumptions are also made for a hard rock squat pillar equation with the Hedley and Grant exponents, the resulting squat pillar formula is given as

$$\sigma_{hard\ rock} = KV^{-0.0833}R_0^{0.6667}\left\{\frac{0.6667}{\varepsilon}\left[\left(\frac{R}{R_0}\right)^\varepsilon - 1\right] + 1\right\} \quad \text{[A14]}$$

And if the calibrated K-value for UG2 is adopted (Oates and Malan, 2023):

$$\sigma_{UG2} = 75 \cdot V^{-0.0833}R_0^{0.6667}\left\{\frac{0.6667}{\varepsilon}\left[\left(\frac{R}{R_0}\right)^\varepsilon - 1\right] + 1\right\}\ MPa \quad \text{[A15]}$$